

Early results from GLASS-JWST XVI: Discovering a bluer $z \sim 4 - 7$ Universe through UV slopes

THEMIYA NANAYAKKARA,¹ KARL GLAZEBROOK,¹ COLIN JACOBS,¹ ANDREA BONCHI,² MARCO CASTELLANO,³
ADRIANO FONTANA,³ CHARLOTTE MASON,^{4,5} EMILIANO MERLIN,³ TAKAHIRO MORISHITA,⁶ DIEGO PARIS,³ MICHELE TRENTI,^{7,8}
TOMMASO TREU,⁹ ANTONELLO CALABRÒ,¹⁰ KRISTAN BOYETT,^{7,8} MARUSA BRADAC,^{11,12} NICHIA LEETHOCHAWALIT,^{7,8,13}
DANILO MARCHESINI,¹⁴ PAOLA SANTINI,¹⁰ VICTORIA STRAIT,^{15,16} EROS VANZELLA,¹⁷ BENEDETTA VULCANI,¹⁸ XIN WANG,¹⁹ AND
LILIAN YANG²⁰

¹Centre for Astrophysics and Supercomputing, Swinburne University of Technology, PO Box 218, Hawthorn, VIC 3122, Australia

²Space Science Data Center, Italian Space Agency, via del Politecnico, 00133, Roma, Italy

³INAF - Osservatorio Astronomico di Roma, via di Frascati 33, 00078 Monte Porzio Catone, Italy

⁴Cosmic Dawn Center (DAWN)

⁵Niels Bohr Institute, University of Copenhagen, Jagtvej 128, 2200 København N, Denmark

⁶IPAC, California Institute of Technology, MC 314-6, 1200 E. California Boulevard, Pasadena, CA 91125, USA

⁷School of Physics, University of Melbourne, Parkville 3010, VIC, Australia

⁸ARC Centre of Excellence for All Sky Astrophysics in 3 Dimensions (ASTRO 3D), Australia

⁹Department of Physics and Astronomy, University of California, Los Angeles, 430 Portola Plaza, Los Angeles, CA 90095, USA

¹⁰INAF Osservatorio Astronomico di Roma, Via di Frascati 33, 00078 Monte Porzio Catone, Rome, Italy

¹¹University of Ljubljana, Department of Mathematics and Physics, Jadranska ulica 19, SI-1000 Ljubljana, Slovenia

¹²Department of Physics and Astronomy, University of California Davis, 1 Shields Avenue, Davis, CA 95616, USA

¹³National Astronomical Research Institute of Thailand (NARIT), Mae Rim, Chiang Mai, 50180, Thailand

¹⁴Department of Physics and Astronomy, Tufts University, 574 Boston Ave., Medford, MA 02155, USA

¹⁵Cosmic Dawn Center (DAWN), Denmark

¹⁶Niels Bohr Institute, University of Copenhagen, Jagtvej 128, DK-2200 Copenhagen N, Denmark

¹⁷INAF – OAS, Osservatorio di Astrofisica e Scienza dello Spazio di Bologna, via Gobetti 93/3, I-40129 Bologna, Italy

¹⁸INAF Osservatorio Astronomico di Padova, vicolo dell'Osservatorio 5, 35122 Padova, Italy

¹⁹Infrared Processing and Analysis Center, Caltech, 1200 E. California Blvd., Pasadena, CA 91125, USA

²⁰Kavli Institute for the Physics and Mathematics of the Universe, The University of Tokyo, Kashiwa, Japan 277-8583

Submitted to ApJL

ABSTRACT

We use the GLASS-JWST Early Release Science NIRCcam parallel observations to provide a first view of the UV continuum properties of NIRCcam/ $F444W$ selected galaxies at $4 < z < 7$. By combining multiwavelength NIRCcam observations, we constrain the UV continuum slope for a sample of 401 galaxies with stringent quality controls. We find that $> 99\%$ of the galaxies are blue star-forming galaxies with very low levels of dust ($A_{v\beta} \sim 0.01 \pm 0.33$). We find no statistically significant correlation for UV slope with redshift or UV magnitude. However, we find that in general galaxies at higher redshifts and fainter UV magnitudes have steeper UV slopes. We find a statistically significant correlation for UV slope with stellar mass, with galaxies with higher stellar mass showing shallower UV slopes. Individual fits to some of our galaxies reach the bluest UV slopes of $\beta \sim -3.1$ allowed by stellar population models used in this analysis. Therefore, it is likely that stellar population models with higher amount of Lyman continuum leakage, AGN effects, and/or Population III contributions are required to accurately reproduce the rest-UV and optical properties of some of our bluest galaxies. This dust-free early view confirms that our current cosmological understanding of gradual mass + dust buildup of galaxies with cosmic time is largely accurate to describe the $\sim 0.7 - 1.5$ Gyr age window of the Universe. The abundance of a large population of UV faint dust-poor systems may point to a dominance of low-mass galaxies at $z > 6$ playing a vital role in cosmic reionization.

1. INTRODUCTION

In the current cosmological picture we expect the first galaxies to emerge $\sim 200 - 300$ Myrs after the Big Bang (e.g. Bromm & Yoshida 2011). These galaxies would rapidly buildup their stellar masses driving the chemical evolutionary

processes of the Universe (e.g. Madau & Dickinson 2014; Dayal & Ferrara 2018). Dust/metals produced as end products of stellar evolution in the early galaxies provide key constraints to how cosmic star-formation would have evolved in the first ~ 3 billion years of the Universe (e.g. Stark 2016).

Thus, establishing a relationship between dust and luminosity in the early Universe from UV bright to faint galaxies would provide tight constraints to galaxy evolution and cosmology (e.g. Naidu et al. 2019; Bouwens et al. 2021, 2022b; Finkelstein et al. 2022; Le Reste et al. 2022; Leethochawalit et al. 2022).

Previous *Hubble Space Telescope* (*HST*) and *Spitzer* observations have been able to detect galaxies in the early Universe shedding light on early cosmic processes (see Bradač (2020) for a review, also Stefanon et al. (2021); Strait et al. (2021); Bouwens et al. (2022a); Finkelstein et al. (2022)). These observations have limitations that hinder their diagnostic power in the early Universe. For example, *HST* observations probe the rest frame UV which may be biased towards young stellar populations unobscured by dust while *Spitzer* can only provide constraints on emission lines or strong spectral features like Balmer breaks (e.g. Stefanon et al. 2022).

Spectroscopic observations of high- z sources with Ly- α provide additional galaxy constraints on gas and dust geometries (e.g. Oesch et al. 2015; Matthee et al. 2018; Jung et al. 2019), albeit with limitations (Leonova et al. 2021; Endsley & Stark 2022). Atacama Large Millimeter/submillimeter Array (ALMA) has been successful in detecting large numbers of sources at $z > 6$ in dust emission with high-efficiency (e.g. Hashimoto et al. 2019; Bouwens et al. 2022c), but galaxy selections for ALMA followup are strongly biased toward UV bright sources (e.g. Bouwens et al. 2022c). Thus, even with recent advancements, the formation timescales of galaxies in the early Universe and their UV luminosity, mass, and dust evolution are not well constrained (Dayal et al. 2022; Finkelstein et al. 2022; Tacchella et al. 2022).

The launch of the *James Webb Space Telescope* (*JWST*) opened up a new window for exploring galaxy evolution in the early Universe. With *JWST*/NIRCam NIR $5\mu\text{m}$ selection (*F444W*), *JWST* can obtain a diverse sample of galaxies in rest-frame optical wavelengths (e.g., Jacobs et al. 2022; Yang et al. 2022a) at $z \sim 4 - 7$. In this analysis we use *JWST* NIRCam (Burriesci 2005) parallel observations from the GLASS-*JWST* survey (Treu et al. 2022) to explore the relationship between UV magnitude and UV slope for galaxies between $z \sim 4 - 7$.

The rest-UV slope is a common indicator for dust attenuation and has been used to explore the buildup of dust in the $z \sim 2 - 10$ Universe (e.g. Reddy et al. 2018). While the UV slope could also be degenerate with metallicity and star-formation history (SFH, e.g. Bouwens et al. 2016b), at fixed UV luminosity galaxies with redder UV slopes have been shown to be dustier compared to their bluer counterparts (Reddy et al. 2018). Additionally, at lower metallicities the indications are that galaxies prefer steeper attenuation curves (Reddy et al. 2018). This means that sight lines of young blue stars in low metallicity galaxies have more dust.

While significant evidence for dust has been hinted by recent ALMA detections, the UV slope evolution between $z \sim 4 - 10$ with UV luminosity is still unclear (e.g. Wilkins et al. 2016; Roberts-Borsani et al. 2022). Studies of UV fainter galaxies (up to $m_{UV} \sim -14$) are largely from *Hubble*

frontier fields, boosted by lensing magnifications (e.g. Yang et al. 2022b), but limited to small volumes. At brighter magnitudes ($m_{UV} \gtrsim -18$), comparisons between field and cluster (lensed) sample UV slopes are found to be largely consistent (Bouwens et al. 2021, 2022b; Yang et al. 2022b).

With GLASS-*JWST* rest-frame optical selection we can constrain the UV slopes of UV faint/red galaxies to investigate whether galaxies are faint due to presence of large amounts of intervening dust or whether they are intrinsically faint in UV due to low star-formation. While Lyman-break galaxies with redder UV slopes of $\beta \sim -1$ have been spectroscopically confirmed at $z \sim 7$ (Smit et al. 2018), we do not have strong constraints of the true abundance of such galaxies. The presence of UV faint high-mass galaxies with shallow UV slopes could lead to significant implications to mass buildup of galaxies at $z > 4$.

In Section 2, we describe our sample selection and UV slope calculation process. In Section 3, we interpret our observations in terms of UV luminosity and dust buildup in the early Universe. Finally, in Section 4 provide a summary of our results and discuss how future surveys would provide tighter constraints to the our cosmological understanding. Unless otherwise stated, we assume a Chabrier (2003) Initial Mass Function (IMF) and a cosmology with $H_0 = 70$ km/s/Mpc, $\Omega_\Lambda = 0.7$ and $\Omega_m = 0.3$. All magnitudes are expressed using the AB system (Oke & Gunn 1983).

2. SAMPLE SELECTION AND UV SLOPE MEASUREMENTS

Our sample is based on the *JWST* GLASS Early Release Science Program Parallel NIRCam observations (Merlin et al. 2022) Stage 1 Data Release (Paris et al. 2023). The observations used here were obtained on 28-29th of June and 10-11th of November 2022 using NIRCam filters *F090W*, *F115W*, *F150W*, *F200W*, *F277W*, *F356W*, *F444W*. The data was reduced using the latest NIRCam calibration files (`cjwst_1014.pmap` to `cjwst_1019.pmap`) provided by STScI. The *F444W* band was selected for source detection and all images were point-spread function (PSF) matched to this band producing a catalog reaching typical $5\text{-}\sigma$ depths of ~ 30.2 mag in all bands. Additionally, *HST* *F606W*, *F775W*, *F814W*, *F435W*, *F105W*, *F125W*, *F140W*, and *F160W* bands and *JWST*/NIRcam *F410M* bands (Bezanson et al. 2022) were folded in where available over the GLASS-*JWST* parallel field (Treu et al. 2022). More details on the observations, data reduction, and catalog generation can be found in Paris et al. (2023).

For the analysis presented in this paper, we required the selected sample to be covered in both rest-frame UV and optical wavelengths in the 7 GLASS-*JWST* NIRCam bands. The rest-frame UV coverage allows us to investigate the accuracy of the best fit spectral energy distribution (SED) shape with the observed photometry. The rest-frame optical coverage includes the Balmer break and strong emission lines such as $H\alpha$ and $[\text{OIII}]\lambda 5007$. Therefore, our final redshift selection for this work is between $4 < z < 7$. Figure 1 shows the observed band coverage for galaxies in this redshift window

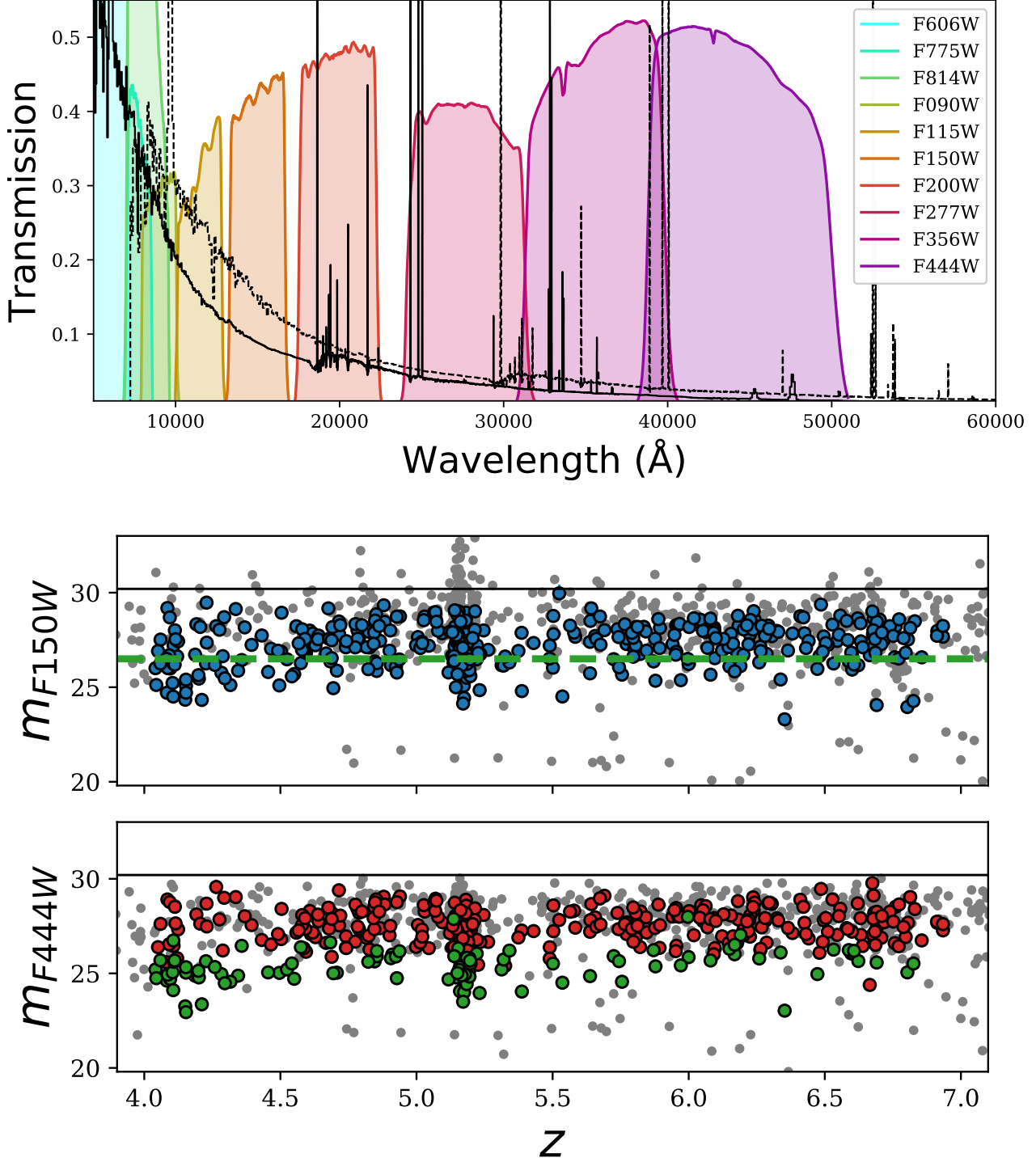


Figure 1. Top: JWST/NIRCam filter coverage of the GLASS-JWST Early Release Science Program observations. In total, observations are obtained over seven NIR filters reaching a 5- σ depth of $m \sim 30.2$. We also show an example EAZY template of a galaxy at $z = 4.0$ (solid lines) and $z = 7.0$ (dashed lines), the lower and upper z limits used in our analysis. With this selection, all our galaxies have rest-frame UV and optical coverage which enables stronger constraints to the overall shape of the SED. A majority of the GLASS-JWST NIRCam parallel field is also covered by *HST* F606W, F775W, and F814W bands; their filter coverage is also shown here. **Bottom:** Photometric properties of the sample used in our analysis. We show the magnitude vs redshift distribution of our galaxies in the (**Bottom Top:** F150W) and (**Bottom Lower:** F444W) bands observed by our survey. The grey dots are the galaxies removed from our analysis based on the stringent quality cuts outlined in Section 2. The horizontal solid line is the nominal 5- σ detection level of $m = 30.2$ for GLASS-JWST NIRCam parallel field. The horizontal green dashed line in the F150W panel is the F150W < 26.4 3DHST survey detection limit (Skelton et al. 2014). We assume that the band pass of HST WFC3/F160W filter is \sim similar to that of the JWST NIRCam/F150W filter. Galaxies that were detectable in 3DHST are marked as green circles in the F444W panel. We note that the XDF detection limit of ~ 29.8 (Bouwens et al. 2014) is similar to that of GLASS-JWST NIRCam parallel field. The typical error bars for most galaxies are smaller than the marker size.

along with additional *HST* data we have obtained over the field (Paris et al. 2023).

We ran the photometric redshift fitting code `EaZY` (Brammer et al. 2008) using the `eazypy` python wrapper¹ to derive photometric redshifts and rest-frame colors for the Paris et al. (2023) catalogue. The total flux measured in 3FWHM PSF matched NIRCam and WFC3 image apertures were selected for this purpose. We used the `tweak_fspqs_QSF_12_v3_newtemplates_Lya_Reduced.param` templates presented in Larson et al. (2022) with `EaZY` to derive the photometric redshifts and rest-frame colors. These templates are derived using FSPS (Conroy et al. 2010) and BPASS (Eldridge et al. 2017) stellar population models and `CLOUDY` (Ferland et al. 2017) photoionisation code and are ideal to describe $z \sim 4 - 7$ galaxies². More information on the models can be found in Larson et al. (2022). For each object, we used the maximum likelihood redshift estimated by `eazypy` as the photometric redshift. Based on 173 secure VLT/MUSE spectroscopic redshifts obtained over the GLASS-JWST field (G. B. Caminha et al., in prep), we derived a photometric redshift accuracy (as defined by Nanayakkara et al. 2016; Straatman et al. 2016) of $\sim 3\%$. When we include the full Paris et al. (2023) catalogue (cluster + GLASS-JWST parallel field) with 379 secure spectroscopic redshifts, the photometric redshift accuracy increase to $\lesssim 2\%$. We also stack the $P(z)$ distributions of $4 < z < 7$ galaxies used for our analysis and find that there is $\sim 87\%$ probability (Nanayakkara et al. 2016) for our sample to lie within this redshift window. We further perform mock GLASS-JWST observations of 5000 galaxies using JAGUAR simulations (Williams et al. 2018) and find that the input redshift can be recovered at the $\sim 2\%$ accuracy.

GLASS-JWST Stage 1 data release contains 24389 objects (Paris et al. 2023). This includes the GLASS-JWST ERS footprint (Treu et al. 2022), the UNCOVER imaging over the ABELL 2744 cluster (Bezanson et al. 2022), and additional JWST imaging from JWST DDT 2756 (PI W. Chen). We select 9272 of galaxies that fall within the GLASS-JWST ERS footprint from the Paris et al. (2023) catalogue for our analysis, out of which 1024 objects were in the redshift window of interest, $4 < z < 7$.

We further pruned this sample by applying stringent quality cuts as follows. First we required galaxies to be detected with a signal to noise (S/N) > 5 in at least 4 photometric bands. This resulted in a sample of 587 galaxies which were detected in a majority of the GLASS-JWST filters. We then visually inspected all the `EaZY` fit SEDs of the galaxies to determine that there were no failed fits. We defined a fit as a failure if a majority of the observed photometric data points did not agree with the template derived flux within photometric errors, i.e. $1-\sigma$ outliers. Only two galaxies fell into this criteria. We further investigated the redshift probability distribution of the galaxies and removed sources that

had $> 50\%$ of the maximum likelihood value at a different redshift. This resulted in a sample of 487 galaxies. Most galaxies that are removed from the sample lie on the redshift range with the highest number of detections ($z \sim 4.5 - 5.5$). Finally, we investigated cutout images of our sample in all the JWST filters used in our analysis and removed sources that were spurious, i.e. sources at the edges of the detectors, sources contaminated with bright neighbors, fragments of stellar spikes, misidentified stars (see Merlin et al. (2022) for details). These stringent cuts resulted in 401 galaxies with high quality photometry and SED fits.

The magnitude distribution of our final sample in the bluest ($F150W$) and reddest ($F444W$) filters as a function of redshift is shown by Figure 1. There is a high abundance of galaxies at $z \sim 5.1$, but apart from that the redshift distribution is quite flat. We find that most galaxies removed by our quality cuts are also at $z \sim 5.1$. Galaxies span a similar range in magnitude in the redder $F444W$ filter ($m_{median} = 27.1 \pm 1.3$) and bluer $F150W$ filters ($m_{median} = 27.4 \pm 1.1$). We also show the $WFC3/F160W = 26.4$ $5-\sigma$ detection level of the 3DHST GOODS-S catalogue (Skelton et al. 2014) in Figure 1. GLASS-JWST is several magnitudes deeper compared to 3DHST and reaches similar detection levels of the deepest imaging in the Hubble eXtreme Deep Field (XDF) obtained by *HST* ($WFC/F160W$ $5-\sigma \sim 29.8$ Bouwens et al. 2014). The faint galaxies that are not detected by 3DHST $\sim 1.5\mu m$ are also faint in the $F444W$ band. This suggest that with the GLASS-JWST $F444W$ selection, we are simply obtaining fainter galaxies that would have otherwise been missed by shallower surveys.

We use the best-fit `EaZY` SEDs to compute the UV slope and UV magnitude of our sample similar to the process outlined by Nanayakkara et al. (2020). We first define a box car filter between $\Delta\lambda = 1400 - 2000\text{\AA}$ and compute the UV magnitude from the `EaZY` best-fit SEDs. Next, for each SED we select a wavelength window between $\Delta\lambda = 1400 - 2000\text{\AA}$ and mask out emission line regions within this window following masks outlined by Calzetti et al. (1994). We then use the masked SEDs to compute the UV continuum slope β by fitting a power-law function using `lmfit` (Newville et al. 2014). We found a single power law to be an accurate description to the UV slopes of all the galaxies in our sample.

We use the JAGUAR mock galaxy catalogue (Williams et al. 2018) to investigate the robustness of our UV slope measurements. We select 50,000 galaxies randomly from the JAGUAR catalogue that satisfy the GLASS-JWST $F444W$ selection. We then perform quality controls to the mock data similar to what we did for the real data in the same filters. The final sample contains 307 galaxies. The intrinsic UV slope β reported by Williams et al. (2018) is recovered with a median offset of only 0.02 ± 0.11 . Thus, our process can recover the UV slopes of galaxies at high accuracy.

We present the `EaZY` derived rest-frame $u_s - g_s$ vs $g_s - i_s$ colors for our sample in Figure 2. This color space has been shown to be effective in distinguishing between quiescent and star-forming galaxies (Antwi-Danso et al. 2022) and is

¹ <https://eazy-py.readthedocs.io>

² <https://ceers.github.io/LarsonSEDTemplates>

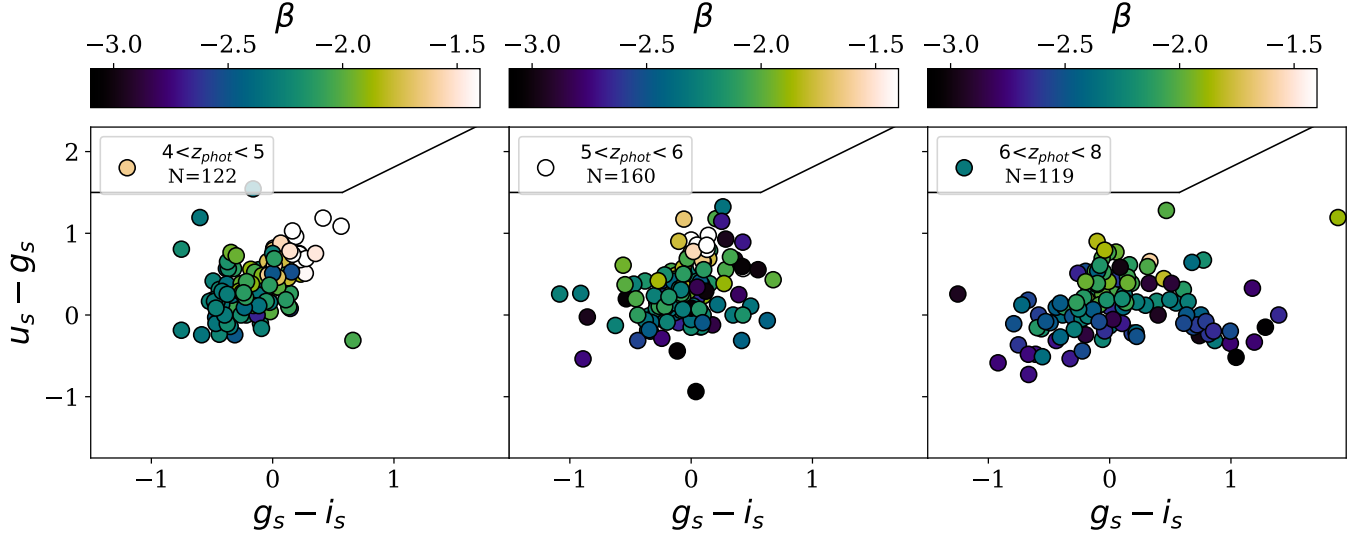


Figure 2. The Rest-frame $u_s - g_s$ vs $g_s - i_s$ (ugi) color distribution (Antwi-Danso et al. 2022) of our sample. We divide the sample into three redshift bins as annotated in the figures and are color coded based on the UV slope β . Almost all galaxies in our sample fall in the star-forming region of the ugi color space. In general galaxies that have bluer ugi colors also show steeper UV slopes.

an improvement over the rest-frame $U - V$ vs $V - J$ colors used at lower redshifts (Williams et al. 2009; Schreiber et al. 2018b). Based on our photometric redshifts, most of the galaxies in our sample fall in the blue star-forming region. There is one galaxy that falls at the edge between star-forming and quiescent region. Galaxies that have shallower UV slopes in general show redder $u_s - g_s$ and $g_s - i_s$ colors. We further compare the differences in $u_s - g_s$ and $g_s - i_s$ colors of galaxies selected by our NIRCam/ $F444W$ selection and 3DHST $WFC3/F160W < 26.4$ selection. We find that there is no significant difference between the color distributions of these two samples. This confirms that our selection is simply targeting fainter galaxies with similar underlying distribution in $u_s - g_s$ and $g_s - i_s$ colors. i.e. we are not finding a hidden population of red-dusty sources with the rest-frame $F444W$ selection. We note that at our highest redshift bin, the i_s band falls out of our $F444W$ filter. Therefore, the rest-frame color here is not directly constrained by the observed photometry. In Figure 3 we show EAZY best-fit SEDs of a representative sample of galaxies presented in our analysis.

We compute stellar masses for our sample using *fast++* (Schreiber et al. 2018c) at the EAZY best-fit redshift. We use Bruzual & Charlot (2003) stellar population models with a Chabrier (2003) IMF, a truncated SFH with a constant and an exponentially declining SFH component, and a Calzetti et al. (2000) dust law. We further derive stellar masses based on non-parametric SFHs (Leja et al. 2019a) using *Prospector* (Johnson et al. 2021) SED fitting similar to Leja et al. (2019b) analysis. The stellar masses derived by *Prospector* includes emission line contribution to observed photometry. We find that the stellar masses between *fast++* and *Prospector* agree within the expected ~ 0.3 dex uncertainty (Conroy 2013; Leja et al. 2019b).

In Figure 4, we show the relationship of the UV continuum slope with redshift, UV magnitude, and stellar mass. In Table 1 we tabulate the binned values observed for these three relationships. While we provide a qualitative description of our relationships, we refrain from quantifying them until after we conduct a thorough analysis of inherent biases associated with UV slope measurements at these redshifts (Finkelstein et al. 2012; Dunlop et al. 2013; Bouwens et al. 2014) in future work.

The UV slope of galaxies does not show any statistically significant correlation (parameterized by the Spearman correlation coefficient (Spearman 1904)) with redshift. However, we find the bluest galaxies in our sample at higher redshifts and reaches a clear minimum value for $\beta \sim -3.1$. This may suggest a limitation on the input SED templates not being able to produce UV slopes blueward of $\lesssim -3.1$.

The UV magnitudes of our sample peaks at $M_{UV} \sim -19$. We observe no statistically significant correlation between UV slope and UV magnitude. Except at the brightest magnitudes, it is clear that some galaxies do reach a clear minimum for UV slopes.

We observe a statistically significant correlation between the UV slope and stellar mass. In general, galaxies with lower stellar masses tend to prefer bluer UV slopes. Given the buildup of stellar mass and dust is correlated, we expect higher stellar mass galaxies to have shallower UV slopes suggesting a higher amount of dust obscuration. We find no correlation between $u_s - g_s$ and $g_s - i_s$ colors with stellar mass in any of the redshift bins. This points to a lack of age/color correlation with stellar mass for our sample. Individual galaxies with stellar masses $\log_{10}(M_*/M_\odot) \lesssim 9$ show evidence of reaching the lower limit for UV magnitude allowed by the templates. We revisit this in Section 3.

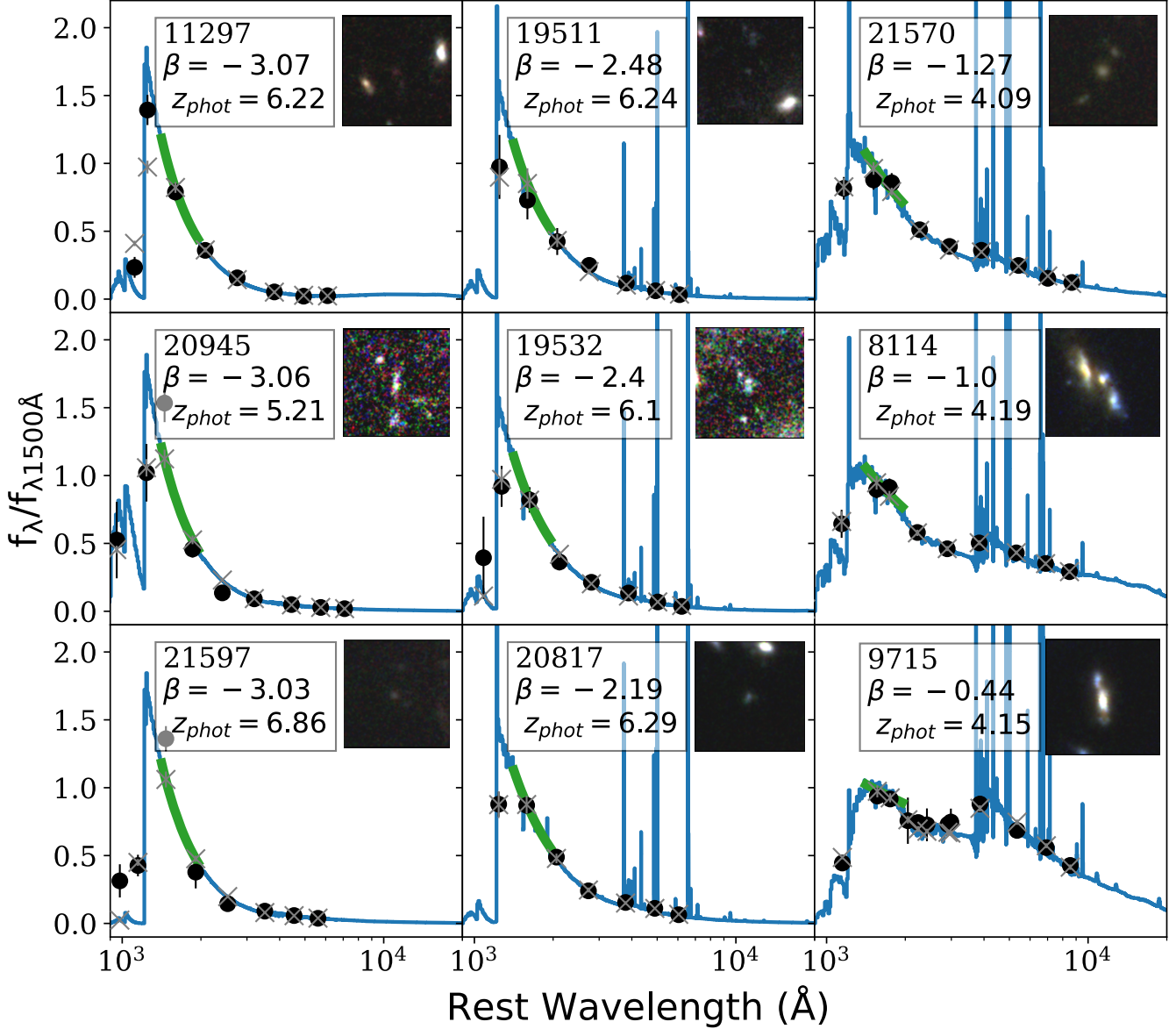


Figure 3. Here we show a representative sample of EAZY best-fit galaxy SEDs used in our analysis. Best-fit EAZY SED photometry and the real observed photometry with their associated errors are shown by crosses and circles, respectively. We show the fit to the UV slope in green. The montages show rest-frame g, r, i color images of the galaxies (see [Jacobs et al. \(2022\)](#) for details). The text in each panel gives the galaxy ID as in ([Paris et al. 2023](#)) catalogue, the UV slope exponent, and the photometric redshift.

3. THE NATURE OF THE UV SLOPES IN THE EARLY UNIVERSE

The UV slope of a galaxy is constrained by the observed photometric bands and thus can be considered as a direct observable. Traditionally, the UV slope has been a useful measurement of the dust content in galaxies where dust emission in the infra-red cannot be easily constrained (e.g [Reddy et al. 2006](#)). At a fixed choice of an attenuation curve, the amount of reddening measures the amount of dust between the young blue O and B type stars in a galaxy and its close proximity (e.g. [Calzetti et al. 1994](#); [Meurer et al. 1999](#)). Shallower the

UV slope (i.e. more positive β values), higher the amount of dust obscuration that is expected in galaxies. However, degeneracies between galaxy age, mass, and luminosity could add extra uncertainty in deriving the amount of dust with the UV slope (e.g [Reddy et al. 2010](#); [Casey et al. 2014](#); [Bouwens et al. 2016a](#)). While far-infrared (FIR) detections could help alleviate this tension, the infra-red excess of galaxies at $z > 4$ is challenging to interpret due to the general reliance of a single ALMA detection to derive the total FIR luminosity. Additionally, constraining analysis to ones only with FIR de-

Table 1. Binned values for our galaxies.

Bin range	N_{sources}	Median β	σ_{β}
$4.00 < z < 4.75$	89	-2.08	0.22
$4.75 < z < 5.50$	140	-2.11	0.17
$5.50 < z < 6.25$	91	-2.43	0.20
$6.25 < z < 7.0$	81	-2.30	0.26
$-23.52 < M_{UV} < -20.07$	100	-2.07	0.22
$-20.07 < M_{UV} < -19.22$	100	-2.21	0.29
$-19.22 < M_{UV} < -18.66$	100	-2.27	0.18
$-18.66 < M_{UV} < -17.11$	101	-2.27	0.15
$7.35 < \log_{10}(M_*/M_{\odot}) < 8.20$	99	-2.48	0.17
$8.20 < \log_{10}(M_*/M_{\odot}) < 8.63$	101	-2.29	0.13
$8.63 < \log_{10}(M_*/M_{\odot}) < 9.08$	98	-2.11	0.15
$9.08 < \log_{10}(M_*/M_{\odot}) < 10.36$	103	-1.86	0.24

NOTE— Values computed for the binned samples as shown by Figure 4.

tections biases analysis towards UV bright or heavily dust obscured galaxies (Hodge & da Cunha 2020).

Our analysis is purely based on a $F444W$ magnitude selected sample of galaxies where we have confident $S/N > 5$ detections in at least 4 photometric bands covering both rest-UV and optical wavelengths. The $F444W$ band cover the rest-optical bands for our galaxies; thus can have significant contributions from emission lines and nebular continuum. We have visually inspected all multi band photometric images, SED fits, and the UV slope fits to every galaxy in the sample. Our stringent quality cuts on the EAZY best fit SEDs allow us to gain initial insights to the UV slopes of rest-optical selected galaxies at $4 < z < 7$. However, we caution that the stringent quality cuts imposed on our magnitude selected sample could lead to incompleteness and selection effects. This needs to be modeled in terms of observed photometry of the NIRCcam bands and is out of scope of this letter.

Our sample reaches UV magnitude of $M_{UV} \sim -18$, which is comparable to the *Hubble* blank field data (Bouwens et al. 2022a). A modest amount of lensing magnification is expected to be present in GLASS-JWST NIRCcam parallel fields. In this initial set of papers we neglect the effect and will be revisited after the completion of the campaign. However, we stress that quantities such as the UV slope and colors are unaffected by magnification and therefore our conclusions are robust in that respect.

Bouwens et al. (2014) derived an empirical relationship between UV slope with redshift ($z \sim 4 - 7$) based on deep *HST* data reaching to $M_{UV} = -16.7$. Within our detection levels, we do not observe a clear redshift or UV magnitude evolution of the UV slope for the GLASS-JWST data (Figure 4). Bouwens et al. (2016b) sample is based on infrared detected Lyman-break galaxies (LBGs), thus it is reasonable that these galaxies observe significantly shallower UV slopes compared to our sample. $z < 3$ galaxies (McLure et al. 2018) also show shallower UV slopes compared to our sample, specially at $\log_{10}(M_*/M_{\odot}) > 9.0$.

In Figure 4 we also show the UV slopes of the luminous Ly- α emitters observed by Jiang et al. (2020). Our sample also reach the extreme blue slopes observed in the Jiang et al. (2020) sample. Jiang et al. (2020) finds that the bluer galaxies in their sample with $\beta \sim -2.7$ are challenging to be reproduced with stellar population models. With the recent Larson et al. (2022) templates used in our analysis, we are able to achieve blue UV slopes of ~ -3.1 .

As mentioned in Section 2, our sample at lower masses and higher redshifts reach the bluer $\beta \lesssim -3.1$ limit that is capable to be fit even by the newest generation of EAZY models. This is evident due to the horizontal limit that is observed at the bluer β values in the individual measurements. Even though the SEDs of the very blue slopes are well constrained over multiple filters, it is possible for photometric redshift uncertainties to scatter redder galaxies to have bluer UV slopes. We perform bootstrap resampling of UV slope measurements to constrain the uncertainty associated with the β measurements. For each galaxy, we recompute the SED fit 100 times within $1 - \sigma$ photometric redshift uncertainty bounds defined by the EAZY $P(z)$ distributions. The $1 - \sigma$ scatter of the measured β values are taken as its error, $\Delta\beta$. The median $\Delta\beta$ for our sample is 0.034 ± 0.11 . For galaxies with $\beta < -3.0$, $\Delta\beta = 0.004 \pm 0.03$. Therefore, it is unlikely that the bluest UV slopes in our sample is a result of the redder galaxies being scattered to blue.

We further test PEGASE (Fioc & Rocca-Volmerange 2019) and FSPS (Conroy & Gunn 2010) model templates with EAZY but are unable to resolve the limitation imposed by the templates to the observed UV slopes. It is likely that a combination of Population III templates (as investigated by Bouwens et al. 2010) or models considering UV continuum leakage/AGN effects as discussed by Jiang et al. (2020) could be required to reach bluer UV slopes than what is allowed by the templates used in our analysis. As the goal of this paper series is to demonstrate the capabilities of JWST data in the context of ERS, we defer a complete treatment of the analysis of UV slopes to future work.

In terms of UV magnitude, our galaxies span a large range in $M_{UV} \sim -23$ to ~ -18 . Our sample does not show a statically significant correlation between UV magnitude and the UV slope. However, we refrain from interpreting this further due to selection effects that could have arisen from our bluer filters. While magnitude depths are quite constant across the bands and reach $\gtrsim 30$ th magnitude, $F090W$ being the bluest band is slightly shallower.

Previous works have found conflicting results on the UV magnitude dependence on β (e.g. Finkelstein et al. 2012; Bouwens et al. 2014; Yamanaka & Yamada 2019; Bhatawdekar & Conselice 2021), especially at $z > 6$. Our binned values are largely in agreement with the Bouwens et al. (2014) relation at brighter UV magnitudes. The $z \sim 4$ LBGs in Yamanaka & Yamada (2019) sample shows redder UV slopes compared to our results. The stellar population analysis of LBGs show that they have a young star-forming stellar population with high amounts of dust. From the *ugi* color analysis in Figure 2, we found that GLASS-

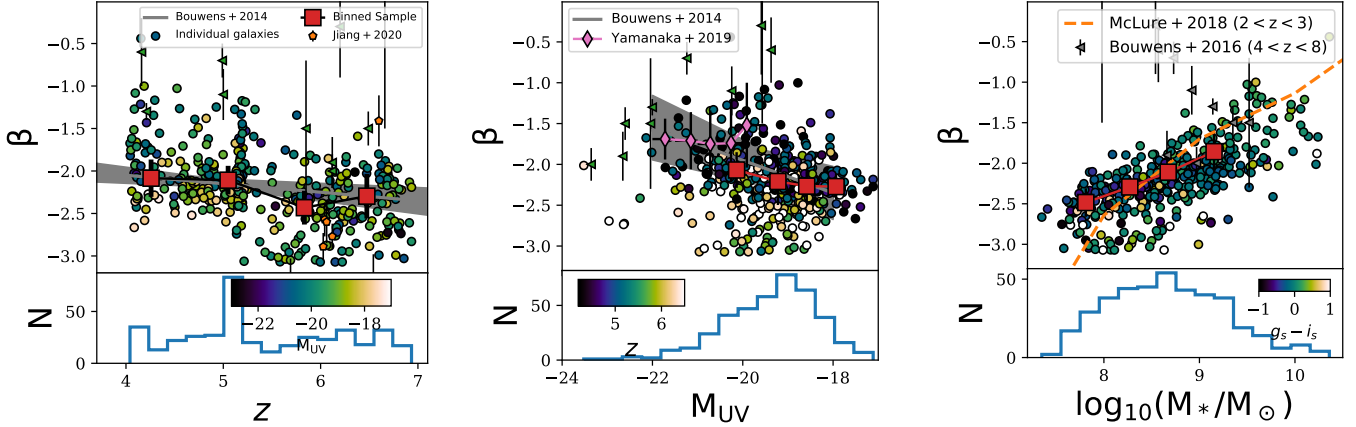


Figure 4. The relationship of the UV slope β with **Left:** redshift (colour coded in terms of UV magnitude), **Center:** rest-frame UV magnitude (colour coded in terms of redshift), and **Right:** stellar mass (colour coded in terms of $g_s - i_s$ color). Galaxies are further binned in each of the three parameters and are shown in the respective panels. Values reported by Bouwens et al. (2016b); Yamanaka & Yamada (2019); Jiang et al. (2020) as well as empirical relationships by Bouwens et al. (2014); McLure et al. (2018) are shown for comparison. We find no statistically significant evolution for β with redshift or UV magnitude, however, we find that β show a dependence on stellar mass. A fraction of galaxies reach $\beta \lesssim -3.1$ suggesting that SED templates with $\beta < -3.1$ are required to accurately predict the rest-UV properties of some galaxies in this epoch.

JWST data are preferentially biased toward blue star-forming systems. Thus, we can rule out significant dust obscuration in our galaxies, and the distinction with Yamanaka & Yamada (2019) is as expected.

In order to determine the dust buildup in the early Universe, the UV slope evolution should be linked with stellar mass and age. As validated by the rest-frame color distributions, we expect the majority of galaxies to be blue, young star-forming systems at these redshifts. Simulations by Pop-ping et al. (2017) show that stellar age also plays a significant role in determining the UV slope. Given sources with redder UV slopes show a bias toward higher masses (Figure 4) we cannot rule out effects from age to our analysis.

Most of our galaxies have blue UV slopes. The expected median attenuation following the Meurer et al. (1999) relation is $A_{v\beta} = 0.01 \pm 0.33$. Therefore, based on our GLASS-JWST NIRCcam $F444W$ selected sample, we expect galaxies at $4 < z < 7$ to be relatively dust-free blue star-forming systems. Within this window the Universe was only $\sim 0.7 - 1.5$ Gyrs old, thus we expect supernovae to be the primary driver of dust buildup in these early systems (Hodge & da Cunha 2020). When compared to $z \sim 2$ K -band selected samples (e.g Shivaie et al. 2018; Nanayakkara et al. 2020), the UV slopes observed by our survey are significantly bluer. At later times, we expect AGB stars to be the dominant dust production mechanisms leading the general population of galaxies to be more dust rich.

We refrain from linking our UV slopes to expected infrared excess (IRX) at $z > 4$. As shown by Bouwens et al. (2016b), the increase of dust temperature with redshift (B  thermin et al. 2015; Schreiber et al. 2018a) and correlations with the assumed dust attenuation curve could add biases to the UV slope-IRX relationship. If galaxies at

early times show harder ionizing spectra with high-energy emission lines (e.g Mainali et al. 2018; Nanayakkara et al. 2019), the relationship between dust production and relationship becomes important. Furthermore, any evolution of the IMF with redshift (Nanayakkara et al. 2017; Sneppen et al. 2022) would add further complications to interpreting the UV slope-dust evolution with redshift.

4. CONCLUSIONS AND FUTURE WORK

We have presented a first view from JWST on the UV slope evolution of NIRCcam $F444W$ selected galaxies at $z \sim 4 - 7$ from our GLASS-JWST program.

- We find that a majority of our galaxies ($> 99\%$) are blue star-forming systems with steep UV slopes.
- We find no statistically significant evolution of the UV slopes with redshift or UV magnitude.
- We find a statistically significant positive correlation of UV slope with stellar mass.
- We find that galaxies with faint UV magnitudes and low stellar masses have bluer UV slopes compared to their UV bright high mass counterparts. This suggest that faint UV systems observed by JWST are blue, low SFR systems.
- We find that some individual measurements of UV slopes hit the bluer limit $\beta \lesssim -3.1$ imposed by the SED templates used in our analysis.

Our observations point to a presence of very blue galaxies in the $z \sim 4 - 7$ Universe. Stellar population models derived using BPASS (Eldridge et al. 2017) and FSPS (Conroy & Gunn 2010) are able to obtain the UV slope properties

of most of our galaxies. Very blue slopes $\beta \sim -3.1$ can be produced by stellar only templates (no nebular continuum contribution) and/or templates with Lyman continuum leakage (Topping et al. 2022). Additionally models that include Population III dust free stars (e.g Bouwens et al. 2010) can also produce very blue UV slopes. Within the context of our work we find that most of the UV slopes of our galaxies can be explained by current stellar population models without the need for any strong exotic effects.

Here we have found that rest-optical selected galaxies at $4 < z < 7$ are preferentially star-forming galaxies with steep UV slopes. Future work should focus on sample selection effects to determine the real number density of extreme blue systems in the early Universe. By combining deep NIRCcam observations between different ERS and JWST Cycle 1 treasury programs, a large representative sample of galaxies at these redshifts could be constructed to analyze the evolution of the UV slope with redshift and UV magnitude. Future spectroscopic observations would be crucial to determine what causes the very blue UV slopes of these galaxies. i.e. high Lyman continuum leakage, extreme low metallicities. Obtaining constraints to the infrared emission and dust temperatures using deep JWST/MIRI and ALMA observations (Schreiber et al. 2018a) planned on JWST JWST Early Release Science (ERS)/Treasury fields and inter-stellar-medium (ISM) conditions from JWST/NIRSpec observations would

add important diagnostic power to determine how the evolution of mass and dust was modulated in the early Universe.

Facility: JWST: (NIRCcam)

This work is based on observations made with the NASA/ESA/CSA James Webb Space Telescope. The data were obtained from the Mikulski Archive for Space Telescopes at the Space Telescope Science Institute, which is operated by the Association of Universities for Research in Astronomy, Inc., under NASA contract NAS 5-03127 for JWST. These observations are associated with program JWST-ERS-1342. We acknowledge financial support from NASA through grant JWST-ERS-1324. T.N., K. G., and C.J. acknowledge support from Australian Research Council Laureate Fellowship FL180100060. MB acknowledges support from the Slovenian national research agency ARRS through grant N1-0238. CM acknowledges support by the VILLUM FONDEN under grant 37459. The Cosmic Dawn Center (DAWN) is funded by the Danish National Research Foundation under grant DNRF140. This project made use of *astropy* (Astropy Collaboration et al. 2018), *matplotlib* (Hunter 2007), and *pandas* (pandas development team 2020).

REFERENCES

- Antwi-Danso, J., Papovich, C., Leja, J., et al. 2022, arXiv e-prints, arXiv:2207.07170. <https://arxiv.org/abs/2207.07170>
- Astropy Collaboration, Price-Whelan, A. M., Sipőcz, B. M., et al. 2018, *AJ*, 156, 123, doi: [10.3847/1538-3881/aabc4f](https://doi.org/10.3847/1538-3881/aabc4f)
- Béthermin, M., Daddi, E., Magdis, G., et al. 2015, *A&A*, 573, A113, doi: [10.1051/0004-6361/201425031](https://doi.org/10.1051/0004-6361/201425031)
- Bezanson, R., Labbe, I., Whitaker, K. E., et al. 2022, arXiv e-prints, arXiv:2212.04026. <https://arxiv.org/abs/2212.04026>
- Bhatawdekar, R., & Conselice, C. J. 2021, *ApJ*, 909, 144, doi: [10.3847/1538-4357/abdd3f](https://doi.org/10.3847/1538-4357/abdd3f)
- Bouwens, R. J., Illingworth, G., Ellis, R. S., et al. 2022a, *ApJ*, 931, 81, doi: [10.3847/1538-4357/ac618c](https://doi.org/10.3847/1538-4357/ac618c)
- Bouwens, R. J., Illingworth, G. D., Ellis, R. S., Oesch, P. A., & Stefanon, M. 2022b, arXiv e-prints, arXiv:2205.11526. <https://arxiv.org/abs/2205.11526>
- Bouwens, R. J., Smit, R., Labbé, I., et al. 2016a, *ApJ*, 831, 176, doi: [10.3847/0004-637X/831/2/176](https://doi.org/10.3847/0004-637X/831/2/176)
- Bouwens, R. J., Illingworth, G. D., Oesch, P. A., et al. 2010, *ApJL*, 708, L69, doi: [10.1088/2041-8205/708/2/L69](https://doi.org/10.1088/2041-8205/708/2/L69)
- , 2014, *ApJ*, 793, 115, doi: [10.1088/0004-637X/793/2/115](https://doi.org/10.1088/0004-637X/793/2/115)
- Bouwens, R. J., Aravena, M., Decarli, R., et al. 2016b, *ApJ*, 833, 72, doi: [10.3847/1538-4357/833/1/72](https://doi.org/10.3847/1538-4357/833/1/72)
- Bouwens, R. J., Oesch, P. A., Stefanon, M., et al. 2021, *AJ*, 162, 47, doi: [10.3847/1538-3881/abf83e](https://doi.org/10.3847/1538-3881/abf83e)
- Bouwens, R. J., Smit, R., Schouws, S., et al. 2022c, *ApJ*, 931, 160, doi: [10.3847/1538-4357/ac5a4a](https://doi.org/10.3847/1538-4357/ac5a4a)
- Bradač, M. 2020, *Nature Astronomy*, 4, 478, doi: [10.1038/s41550-020-1104-5](https://doi.org/10.1038/s41550-020-1104-5)
- Brammer, G. B., van Dokkum, P. G., & Coppi, P. 2008, *ApJ*, 686, 1503, doi: [10.1086/591786](https://doi.org/10.1086/591786)
- Bromm, V., & Yoshida, N. 2011, *ARA&A*, 49, 373, doi: [10.1146/annurev-astro-081710-102608](https://doi.org/10.1146/annurev-astro-081710-102608)
- Bruzual, G., & Charlot, S. 2003, *MNRAS*, 344, 1000, doi: [10.1046/j.1365-8711.2003.06897.x](https://doi.org/10.1046/j.1365-8711.2003.06897.x)
- Burriesci, L. G. 2005, in *Society of Photo-Optical Instrumentation Engineers (SPIE) Conference Series*, Vol. 5904, *Cryogenic Optical Systems and Instruments XI*, ed. J. B. Heaney & L. G. Burriesci, 21–29, doi: [10.1117/12.613596](https://doi.org/10.1117/12.613596)
- Calzetti, D., Armus, L., Bohlin, R. C., et al. 2000, *ApJ*, 533, 682, doi: [10.1086/308692](https://doi.org/10.1086/308692)
- Calzetti, D., Kinney, A. L., & Storchi-Bergmann, T. 1994, *ApJ*, 429, 582, doi: [10.1086/174346](https://doi.org/10.1086/174346)
- Casey, C. M., Scoville, N. Z., Sanders, D. B., et al. 2014, *ApJ*, 796, 95, doi: [10.1088/0004-637X/796/2/95](https://doi.org/10.1088/0004-637X/796/2/95)
- Chabrier, G. 2003, *Publications of the Astronomical Society of the Pacific*, 115, pp. 763. <http://www.jstor.org/stable/10.1086/376392>

- Conroy, C. 2013, *ARA&A*, 51, 393, doi: [10.1146/annurev-astro-082812-141017](https://doi.org/10.1146/annurev-astro-082812-141017)
- Conroy, C., & Gunn, J. E. 2010, *ApJ*, 712, 833, doi: [10.1088/0004-637X/712/2/833](https://doi.org/10.1088/0004-637X/712/2/833)
- Conroy, C., White, M., & Gunn, J. E. 2010, *ApJ*, 708, 58, doi: [10.1088/0004-637X/708/1/58](https://doi.org/10.1088/0004-637X/708/1/58)
- Dayal, P., & Ferrara, A. 2018, *PhR*, 780, 1, doi: [10.1016/j.physrep.2018.10.002](https://doi.org/10.1016/j.physrep.2018.10.002)
- Dayal, P., Ferrara, A., Sommovigo, L., et al. 2022, *MNRAS*, 512, 989, doi: [10.1093/mnras/stac537](https://doi.org/10.1093/mnras/stac537)
- Dunlop, J. S., Rogers, A. B., McLure, R. J., et al. 2013, *MNRAS*, 432, 3520, doi: [10.1093/mnras/stt702](https://doi.org/10.1093/mnras/stt702)
- Eldridge, J. J., Stanway, E. R., Xiao, L., et al. 2017, *PASA*, 34, e058, doi: [10.1017/pasa.2017.51](https://doi.org/10.1017/pasa.2017.51)
- Endsley, R., & Stark, D. P. 2022, *MNRAS*, 511, 6042, doi: [10.1093/mnras/stac524](https://doi.org/10.1093/mnras/stac524)
- Ferland, G. J., Chatzikos, M., Guzmán, F., et al. 2017, *RMxAA*, 53, 385. <https://arxiv.org/abs/1705.10877>
- Finkelstein, S. L., Papovich, C., Salmon, B., et al. 2012, *ApJ*, 756, 164, doi: [10.1088/0004-637X/756/2/164](https://doi.org/10.1088/0004-637X/756/2/164)
- Finkelstein, S. L., Bagley, M., Song, M., et al. 2022, *ApJ*, 928, 52, doi: [10.3847/1538-4357/ac3aed](https://doi.org/10.3847/1538-4357/ac3aed)
- Fioc, M., & Rocca-Volmerange, B. 2019, arXiv e-prints, arXiv:1902.02198. <https://arxiv.org/abs/1902.02198>
- Hashimoto, T., Inoue, A. K., Mawatari, K., et al. 2019, *PASJ*, 71, 71, doi: [10.1093/pasj/psz049](https://doi.org/10.1093/pasj/psz049)
- Hodge, J. A., & da Cunha, E. 2020, *Royal Society Open Science*, 7, 200556, doi: [10.1098/rsos.200556](https://doi.org/10.1098/rsos.200556)
- Hunter, J. D. 2007, *Computing In Science & Engineering*, 9, 90
- Jacobs, C., Glazebrook, K., Calabrò, A., et al. 2022, arXiv e-prints, arXiv:2208.06516. <https://arxiv.org/abs/2208.06516>
- Jiang, L., Cohen, S. H., Windhorst, R. A., et al. 2020, *ApJ*, 889, 90, doi: [10.3847/1538-4357/ab64ea](https://doi.org/10.3847/1538-4357/ab64ea)
- Johnson, B. D., Leja, J., Conroy, C., & Speagle, J. S. 2021, *ApJS*, 254, 22, doi: [10.3847/1538-4365/abef67](https://doi.org/10.3847/1538-4365/abef67)
- Jung, I., Finkelstein, S. L., Dickinson, M., et al. 2019, *ApJ*, 877, 146, doi: [10.3847/1538-4357/ab1bde](https://doi.org/10.3847/1538-4357/ab1bde)
- Larson, R. L., Hutchison, T. A., Bagley, M., et al. 2022, arXiv e-prints, arXiv:2211.10035. <https://arxiv.org/abs/2211.10035>
- Le Reste, A., Hayes, M., Cannon, J. M., et al. 2022, arXiv e-prints, arXiv:2206.06374. <https://arxiv.org/abs/2206.06374>
- Leethochawalit, N., Roberts-Borsani, G., Morishita, T., Trenti, M., & Treu, T. 2022, arXiv e-prints, arXiv:2205.15388. <https://arxiv.org/abs/2205.15388>
- Leja, J., Carnall, A. C., Johnson, B. D., Conroy, C., & Speagle, J. S. 2019a, *ApJ*, 876, 3, doi: [10.3847/1538-4357/ab133c](https://doi.org/10.3847/1538-4357/ab133c)
- Leja, J., Johnson, B. D., Conroy, C., et al. 2019b, *ApJ*, 877, 140, doi: [10.3847/1538-4357/ab1d5a](https://doi.org/10.3847/1538-4357/ab1d5a)
- Leonova, E., Oesch, P. A., Qin, Y., et al. 2021, arXiv e-prints, arXiv:2112.07675. <https://arxiv.org/abs/2112.07675>
- Madau, P., & Dickinson, M. 2014, *ARA&A*, 52, 415, doi: [10.1146/annurev-astro-081811-125615](https://doi.org/10.1146/annurev-astro-081811-125615)
- Mainali, R., Zitrin, A., Stark, D. P., et al. 2018, *MNRAS*, 479, 1180, doi: [10.1093/mnras/sty1640](https://doi.org/10.1093/mnras/sty1640)
- Matthee, J., Sobral, D., Gronke, M., et al. 2018, ArXiv e-prints, arXiv:1805.11621. <https://arxiv.org/abs/1805.11621>
- McLure, R. J., Pentericci, L., Cimatti, A., et al. 2018, *MNRAS*, 479, 25, doi: [10.1093/mnras/sty1213](https://doi.org/10.1093/mnras/sty1213)
- Merlin, E., Bonchi, A., Paris, D., et al. 2022, *ApJL*, 938, L14, doi: [10.3847/2041-8213/ac8f93](https://doi.org/10.3847/2041-8213/ac8f93)
- Meurer, G. R., Heckman, T. M., & Calzetti, D. 1999, *ApJ*, 521, 64, doi: [10.1086/307523](https://doi.org/10.1086/307523)
- Naidu, R. P., Tacchella, S., Mason, C. A., et al. 2019, arXiv e-prints, arXiv:1907.13130. <https://arxiv.org/abs/1907.13130>
- Nanayakkara, T., Glazebrook, K., Kacprzak, G. G., et al. 2016, *ApJ*, 828, 21, doi: [10.3847/0004-637X/828/1/21](https://doi.org/10.3847/0004-637X/828/1/21)
- . 2017, *MNRAS*, 468, 3071, doi: [10.1093/mnras/stx605](https://doi.org/10.1093/mnras/stx605)
- Nanayakkara, T., Brinchmann, J., Boogaard, L., et al. 2019, *A&A*, 624, A89, doi: [10.1051/0004-6361/201834565](https://doi.org/10.1051/0004-6361/201834565)
- Nanayakkara, T., Brinchmann, J., Glazebrook, K., et al. 2020, *ApJ*, 889, 180, doi: [10.3847/1538-4357/ab65eb](https://doi.org/10.3847/1538-4357/ab65eb)
- Newville, M., Stensitzki, T., Allen, D. B., & Ingargiola, A. 2014, LMFIT: Non-Linear Least-Square Minimization and Curve-Fitting for Python, 0.8.0, Zenodo, Zenodo, doi: [10.5281/zenodo.11813](https://doi.org/10.5281/zenodo.11813)
- Oesch, P. A., van Dokkum, P. G., Illingworth, G. D., et al. 2015, *ApJ*, 804, L30, doi: [10.1088/2041-8205/804/2/L30](https://doi.org/10.1088/2041-8205/804/2/L30)
- Oke, J. B., & Gunn, J. E. 1983, *ApJ*, 266, 713, doi: [10.1086/160817](https://doi.org/10.1086/160817)
- pandas development team, T. 2020, pandas-dev/pandas: Pandas, latest, Zenodo, doi: [10.5281/zenodo.3509134](https://doi.org/10.5281/zenodo.3509134)
- Paris, D., Merlin, E., Fontana, A., et al. 2023, arXiv e-prints, arXiv:2301.02179. <https://arxiv.org/abs/2301.02179>
- Popping, G., Puglisi, A., & Norman, C. A. 2017, *MNRAS*, 472, 2315, doi: [10.1093/mnras/stx2202](https://doi.org/10.1093/mnras/stx2202)
- Reddy, N. A., Erb, D. K., Pettini, M., Steidel, C. C., & Shapley, A. E. 2010, *ApJ*, 712, 1070, doi: [10.1088/0004-637X/712/2/1070](https://doi.org/10.1088/0004-637X/712/2/1070)
- Reddy, N. A., Steidel, C. C., Fadda, D., et al. 2006, *ApJ*, 644, 792, doi: [10.1086/503739](https://doi.org/10.1086/503739)
- Reddy, N. A., Oesch, P. A., Bouwens, R. J., et al. 2018, *ApJ*, 853, 56, doi: [10.3847/1538-4357/aaa3e7](https://doi.org/10.3847/1538-4357/aaa3e7)
- Roberts-Borsani, G., Morishita, T., Treu, T., Leethochawalit, N., & Trenti, M. 2022, *ApJ*, 927, 236, doi: [10.3847/1538-4357/ac4803](https://doi.org/10.3847/1538-4357/ac4803)
- Schreiber, C., Elbaz, D., Pannella, M., et al. 2018a, *A&A*, 609, A30, doi: [10.1051/0004-6361/201731506](https://doi.org/10.1051/0004-6361/201731506)
- Schreiber, C., Labbé, I., Glazebrook, K., et al. 2018b, *A&A*, 611, A22, doi: [10.1051/0004-6361/201731917](https://doi.org/10.1051/0004-6361/201731917)
- Schreiber, C., Glazebrook, K., Nanayakkara, T., et al. 2018c, *A&A*, 618, A85, doi: [10.1051/0004-6361/201833070](https://doi.org/10.1051/0004-6361/201833070)

- Shivaei, I., Reddy, N. A., Siana, B., et al. 2018, *ApJ*, 855, 42, doi: [10.3847/1538-4357/aaad62](https://doi.org/10.3847/1538-4357/aaad62)
- Skelton, R. E., Whitaker, K. E., Momcheva, I. G., et al. 2014, *ApJS*, 214, 24, doi: [10.1088/0067-0049/214/2/24](https://doi.org/10.1088/0067-0049/214/2/24)
- Smit, R., Bouwens, R. J., Carniani, S., et al. 2018, *Nature*, 553, 178, doi: [10.1038/nature24631](https://doi.org/10.1038/nature24631)
- Sneppen, A., Steinhardt, C. L., Hensley, H., et al. 2022, *ApJ*, 931, 57, doi: [10.3847/1538-4357/ac695e](https://doi.org/10.3847/1538-4357/ac695e)
- Spearman, C. 1904, *The American Journal of Psychology*, 15, 72. <http://www.jstor.org/stable/1412159>
- Stark, D. P. 2016, *ARA&A*, 54, 761, doi: [10.1146/annurev-astro-081915-023417](https://doi.org/10.1146/annurev-astro-081915-023417)
- Stefanon, M., Bouwens, R. J., Labbé, I., et al. 2022, *ApJ*, 927, 48, doi: [10.3847/1538-4357/ac3de7](https://doi.org/10.3847/1538-4357/ac3de7)
- Stefanon, M., Labbé, I., Oesch, P. A., et al. 2021, *ApJS*, 257, 68, doi: [10.3847/1538-4365/ac2498](https://doi.org/10.3847/1538-4365/ac2498)
- Straatman, C. M. S., Spitler, L. R., Quadri, R. F., et al. 2016, *ApJ*, 830, 51, doi: [10.3847/0004-637X/830/1/51](https://doi.org/10.3847/0004-637X/830/1/51)
- Strait, V., Bradač, M., Coe, D., et al. 2021, *ApJ*, 910, 135, doi: [10.3847/1538-4357/abe533](https://doi.org/10.3847/1538-4357/abe533)
- Tacchella, S., Finkelstein, S. L., Bagley, M., et al. 2022, *ApJ*, 927, 170, doi: [10.3847/1538-4357/ac4cad](https://doi.org/10.3847/1538-4357/ac4cad)
- Topping, M. W., Stark, D. P., Endsley, R., et al. 2022, *ApJ*, 941, 153, doi: [10.3847/1538-4357/aca522](https://doi.org/10.3847/1538-4357/aca522)
- Treu, T., Roberts-Borsani, G., Bradac, M., et al. 2022, *ApJ*, in press, arXiv:2206.07978. <https://arxiv.org/abs/2206.07978>
- Wilkins, S. M., Bouwens, R. J., Oesch, P. A., et al. 2016, *MNRAS*, 455, 659, doi: [10.1093/mnras/stv2263](https://doi.org/10.1093/mnras/stv2263)
- Williams, C. C., Curtis-Lake, E., Hainline, K. N., et al. 2018, *ApJS*, 236, 33, doi: [10.3847/1538-4365/aabcbb](https://doi.org/10.3847/1538-4365/aabcbb)
- Williams, R. J., Quadri, R. F., Franx, M., van Dokkum, P., & Labbé, I. 2009, *ApJ*, 691, 1879, doi: [10.1088/0004-637X/691/2/1879](https://doi.org/10.1088/0004-637X/691/2/1879)
- Yamanaka, S., & Yamada, T. 2019, *PASJ*, 71, 51, doi: [10.1093/pasj/psz024](https://doi.org/10.1093/pasj/psz024)
- Yang, L., Morishita, T., Leethochawalit, N., et al. 2022a, *ApJL*, 938, L17, doi: [10.3847/2041-8213/ac8803](https://doi.org/10.3847/2041-8213/ac8803)
- Yang, L., Leethochawalit, N., Treu, T., et al. 2022b, *MNRAS*, 514, 1148, doi: [10.1093/mnras/stac1236](https://doi.org/10.1093/mnras/stac1236)